HYSAFE SBEP-V20: NUMERICAL PREDICTIONS OF RELEASE EXPERIMENTS INSIDE A RESIDENTIAL GARAGE WITH PASSIVE VENTILATION

Papanikolaou, E.A.[1, 7], Venetsanos, A.G.[1], Heitsch, M.[2], Baraldi, D.[2], Huser, A.[3], Pujol, J.[3], Makarov, D.[4], Molkov, V.[4], Garcia, J.[5] and Markatos, N.[6]

[1] Environmental Research Laboratory, National Centre for Scientific Research Demokritos, Aghia Paraskevi, Attikis, 15310, Greece
venets@ipta.demokritos.gr
[2] European Commission DG-JRC, Institute for Energy - Cleaner Energies Unit, 1755 ZG Petten, The Netherlands
[3] DNV Research and Innovation, Oslo, Norway
[4] HySAFER centre, University of Ulster (UU), Newtownabbey, BT37 0QB, Northern Ireland, UK
[5] Escuela Técnica Superior de Ingenieros Industriales, Universidad Politécnica de Madrid, José Gutiérrez Abascal, 2, E-28006 Madrid, Spain
[6] National Technical University of Athens, School of Chemical Engineering, Zografou, 15780, Greece

ABSTRACT

This work presents the results of the Standard Benchmark Exercise Problem (SBEP) V20 of WP6 of HySAFE Network of Excellence (NoE), co-funded by E.C., in the framework of evaluating the quality and suitability of codes, models and user practices by comparative assessments of code results. The benchmark problem SBEP-V20 is based on release scenarios that were experimentally investigated in the past using helium as a substitute to hydrogen. The aim of the investigations was to determine the ventilation requirements for parking hydrogen fuelled vehicles in residential garages. Helium is released under the vehicle for 2 hours with 7.200 L/hr flow rate. The leak rate corresponds to a 20% drop of the peak power of a 50kW fuel cell vehicle. Three double vent garage door geometries are considered. In each case the vents are located at the top and bottom of the garage door. The vents vary only in height. In the first case, the height of the vents is 2.5 inches, in the second 9.5 inches and in the third 19.5 inches. Five HySAFE partners participated in this benchmark. The following CFD packages with the respective models have been applied to simulate the experiments: ADREA-HF using k-e model by partner NCSRD, FLACS using k-e model by partner DNV, FLUENT using k-e model by partners UPM and UU and CFX using laminar and the low-Re number SST model by partner JRC. This study compares the results predicted by the partners to the experimental measurements at four sensor locations inside the garage with an attempt to assess and validate the performance of the different codes and models. Furthermore, the effect of passive ventilation on the formation of flammable cloud is investigated.

1 INTRODUCTION

A part of the Integrating Activities within the HySafe Network of Excellence (NoE) [1] was the collection of experiments in areas relevant to hydrogen safety for code and model benchmarking. The exercises proposed by the consortium partners were identified as SBEPs which stands for “Standard Benchmark Exercise Problems”. Apart from validating the performance of the codes and models to reproduce the experimental data, a comparative assessment between them was aimed to identify the main priority areas for further development of the codes and models and to provide recommendations for optimal tools and user best practices. In other words, the assessment of the quality and suitability of codes and models and the recommendation of user best practices were the main scope of the SBEPs.

The benchmark problem SBEP V20 is based on release scenarios that have been experimentally investigated in the past by Swain et al. (1998) [2]. Swain et al. (1998) [2] conducted an experimental and CFD research program to determine the ventilation requirements of residential garages to store hydrogen fuelled vehicles. Specifically, the work investigated the suitability of existing garages to store hydrogen fuelled vehicles and the need for any modifications. A full scale model of a single car garage containing a vehicle was used. The experimental facility was located indoors to eliminate wind and outdoor temperature variations. During the course of the experiments and based on the results several modifications were investigated. Initially, the modifications covered natural ventilation which was provided by vents at the garage door whereas a vent located at the ceiling was also investigated. Finally, forced ventilation and a hydrogen detection system were examined. Helium at a leak rate of 7.200 lt/hr located under the car was used as a surrogate to hydrogen for all experiments. The CFD calculations were performed using FLUENT. The calculations showed that the difference in hydrogen and helium concentrations in resembling geometries rarely outgoes 15%. The largest differences occurred during the transient period before steady state and before the highest concentrations were reached. Papanikolaou et al. (2005) [3] presented the results of the simulations of 3 cases of the Swain garage experiments [2] using the standard k-e model. The results were generally in good agreement with the experimental.

Later Swain et al. (1999) [4] performed hydrogen dispersion experiments in simple vented enclosures and associated CFD validation using the FLUENT code. Agranat et al. (2004) [5] simulated the vented hallway experiment using the PHOENICS code and found results similar to the FLUENT code. In the paper of Swain (1998) [6] a comparison of the safety risks of four types of vehicle fuels (hydrogen, natural gas, LPG and gasoline) release inside a single car garage was made using FLUENT code. It was found that only LPG and gasoline produced appreciable volumes of combustible gas. In another work, Breitung et al. (2001) [7] applied the GASFLOW CFD code to calculate the temporal and spatial distribution of hydrogen and applied criteria to evaluate the flame acceleration and detonation potential in an effort to estimate the combustion hazards, due to the boil-off from the cryogenic hydrogen tank of a car in a private garage. In the work of Parsons and Brinckerhoff (2004) [8] facility modifications and associated incremental costs that may be necessary to safely accommodate hydrogen fuel cell vehicles in four support facility case studies (commercial multi-story above-ground parking, commercial multi-story below-ground parking, residential two vehicle garages and commercial maintenance/repair/service station) were evaluated. The methodology applied was also CFD calculations. Paillere et al. (2005) [9] highlighted the importance of using CFD for safety assessment, design of mitigation systems and presented a validation of their in-house code in release, dispersion, combustion and mitigation scenarios. Barley et al. (2007) [10] provided relationships between design variables (vent area, height, discharge coefficient) for buoyancy-driven passive ventilation of H2 from a room. A simplified model was described and a CFD code was used to simulate a typical two-car garage with different H2 leakage rates scenarios. Gupta et al. (2007) [11] provided a detailed experimental information on H2 dispersion inside a full scale unventilated garage. The test cases evaluated the influence of injected H2 volumes and initial conditions on the dispersion and mixing characteristics inside the facility whereas He was used instead of H2. The authors concluded that the risk induced is most strongly affected by the total volume of the released gas rather than by the flow rate. Lowesmith et al. (2007) [12] presented an experimental work of gas (with varied H2/CH4 composition) release inside a ventilated enclosure. Analysis of data and predictions were done with the use of a simple mathematical model. The authors concluded that both buoyancy and wind driven ventilation are important. The paper by Lacome et al. (2007) [13] presents test results of subsonic H2 releases in confined area. A comparison between He and H2 concentrations was also made. The authors stated that He can be used as a substitute to H2 although further experiments are necessary. The paper by Venetsanos et al. (2009) [14] presents a CFD inter-comparison of an experiment inside a garage with 1 g/s H2 vertical release. Pre-test and post-test simulations of 12 organizations using different codes/models were evaluated. Large variation was found in the results during the pre-test phase whereas the variation was significantly reduced in the post-test phase. The paper by Papakonstantinou et al. (2003) [15] presented a simulation work of CO concentration inside a typical central garage with and without mechanical ventilation. The results showed that the numerical

solutions were very effective for ventilation and design purposes. Duci et al. (2004) [16] presented simulations of CO inside a typical garage for three different ventilation rates and concluded that the CFD calculations can be obtained quickly and economically with considerable confidence. The review shows not only the experimental work of H2 releases focused in enclosures (such as garages) but also the importance of using CFD codes as a tool for risk assessment, estimation of hazards and as basis of suggestions to the design requirements of a garage to safely accommodate hydrogen vehicles. On the other hand the scenarios often include slow flow conditions (laminar or transitional), for which the choice of a model is not trivial. The selection of grid resolution and boundary conditions is another issue that needs to be addressed. Consequently, the development of CFD practice guidelines, based on extensive validation work for scenarios is crucial.

This work focuses on the helium experiments by Swain et al. [2]. Three of these tests were selected as benchmark problem SBEP V20. Five HySAFE partners participated in this benchmark with different CFD packages and approaches. This study compares the results predicted by the partners to the experimental data at four sensor locations inside the garage with an attempt to assess and validate the performance of the different codes and models. Furthermore, the structure of the flow field and the effect of passive ventilation on the formation of flammable cloud are investigated.

2 EXPERIMENTAL DESCRIPTION

The experimental facility represents a full scale single car garage with two vents on the door. Different vent garage door geometries were tested. In all cases the vents extended the width of the garage door. A full-scale plywood model vehicle was placed inside the garage. All testing was done with helium as a surrogate to hydrogen. The helium flow rate was 7.200 Lt/hr and the release lasted 2 hours. The leak location was at the bottom of the vehicle in the front part and centered. The sensors were located at the four corners of the garage. Three of the Swain tests were selected as benchmark problem SBEP V20, Case 1 (2.5 inches vent height), Case 2 (9.5 inches vent height) and Case 3 (19.5 inches vent height). Figure 1 shows the geometry of the experimental facility and the location of the leak, the vents and the 4 sensors. The geometrical details of the facility can be found in [3]. No information was available about the uncertainties of the measurements. Some of the reported He concentrations were very small which usually involves relatively high measurement errors.

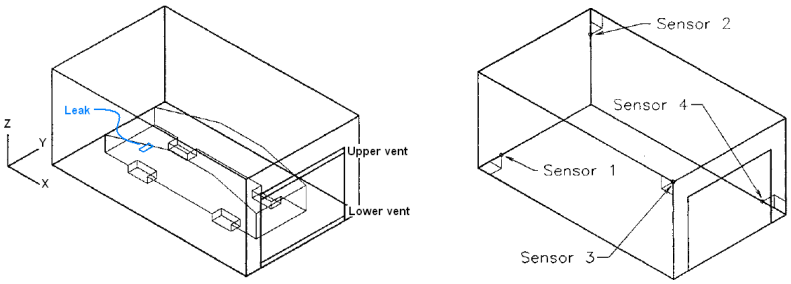

Figure 1: Geometry of the experimental facility and location of sensors

3 BENCHMARK DESCRIPTION

Five HySAFE partners participated in this benchmark with different CFD packages and approaches. The main characteristics of the modeling approach of each participant are given in Table 1 and Table 2. The tables give the details of the modeling strategy that was adopted for the results that were submitted as “final results” for inter-comparison. Additionally, partners DNV, JRC and NCSRD performed grid independence tests. DNV and JRC also used different models to examine whether they affect the results. DNV examined two different boundary conditions, the “symmetry” and “nozzle” and different time steps. UU examined two different time steps for one case. Finally, NCSRD and DNV examined the effect of the domain size. These issues will be discussed in the following section.

Table 1: Main characteristics of the codes/models used by the participants

Participant	CFD Code	Model	Discretization schemes C: convective scheme, T: temporal scheme
DNV	FLACS 9 [17]	k-ε standard σ_κ=1.0, σ_ε=1.3, σ = 0.7	SIMPLE for pressure-velocity coupling C: 2nd order "kappa" scheme (blends upwind and central difference) T: 1st order backward Euler
JRC	CFX 11 SP1 [18]	Laminar, buoyant	C: 2nd order (high resolution) T: 2nd order backward Euler
NCSRD	ADRA-HF [19]	k-ε standard with buoyancy effects σ_κ=1.0, σ_ε=1.3, σ = 0.72	C: 1st order upwind T: 1st order fully implicit
UPM	FLUENT [20]	k-ε standard	C: 2nd order upwind T: 1st order implicit
UU	FLUENT	k-ε standard with buoyancy effects	SIMPLE for pressure-velocity coupling PRESTO! discretization for pressure terms C: PowerLaw T: 2nd order accurate time stepping

Table 2: Main characteristics of the codes/models used by the participants

Participant	Domain and Grid Characteristics	Time step, CPU time, computer	Initial and boundary conditions
DNV	Extended domain by 10% garage length in x-direction (Case 1 and 2), extended by 55% garage length in x-direction (Case 3) Cartesian grid Case 1: 13.000 cells (40x13x25), 0.1m in X, 0.2m in Y, 0.06m in Z minimum cell size, 0.31m in X, 0.38m in Y, 0.18m in Z maximum cell size Case 2: 14.560 cells (40x13x28), 0.1m in X, 0.2m in Y, 0.04m in Z minimum cell size, 0.31m in X, 0.38m in Y, 0.18m in Z maximum cell size Case 3: 16.575 cells (51x13x25), 0.1m in X, 0.2m in Y, 0.06m in Z minimum cell size, 0.28m in X, 0.38m in Y, 0.18m in Z maximum cell size	Time step: 0.01 sec System clock time: 100, 230 and 100 hr for Case 1, 2, and 3 2CPU DELL Intel Xeon 2.66GHz (code runs with 1 CPU), 2Gb RAM	Temperature: 20ºC, Jet inlet: $3.284 \cdot 10^{-4}$ kg/s, 0.02 m^2 jet area, "Nozzle" boundary condition to all computational boundaries (ambient pressure and zero gradient to rest of variables) Ground and garage walls: No slip with log law
JRC	Extended domain by almost 50% and 100% in the x and z directions 418.945 tetrahedral cells (81.374 nodes)	Time adaptive method with automatic time step selection between 0.1 and 1 sec (average	Temperature: 15ºC, Jet inlet: $3.4 \cdot 10^{-4}$ kg/s, 0.1 m/s Boundary conditions at open surfaces: For sidewalls:

		time step: 0.25sec). System clock time: 106 hr (typical) 8 Intel Xeon 3GHz	symmetry plane For top: opening (flow possible in all directions) For Front: Outlet (flow only outwards) For Bottom and back side: Wall
NCSRD	Symmetry assumption (half garage), extended domain by 1 garage length, ½ garage width and 1 garage height in x, y and z-direction Cartesian grid Case 1: 31.411 cells (71x25x34), 18.661 cells inside garage, 0.1m in X, 0.1m in Y, 0.102m in Z minimum cell size, 0.147m in X, 0.139m in Y, 0.149m in Z maximum cell size with 1.01-1.02 expansion ratio inside garage Case 2: 36.411 cells (71x25x34), 18.661 cells inside garage, 0.1m in X, 0.1m in Y, 0.102m in Z minimum cell size, 0.147m in X, 0.139m in Y, 0.149m in Z maximum cell size with 1.01-1.02 expansion ratio inside garage Case 3: 22.364 cells (59x23x32), 12.796 cells inside garage, 0.125m in X, 0.125m in Y, 0.102m in Z minimum cell size, 0.17m in X, 0.14m in Y, 0.157m in Z maximum cell size with 1.01-1.02 expansion ratio inside garage	Maximum allowed time step: 10^{-1} sec System clock time: 17, 15 and 10 hr for Case 1, 2, and 3 PC Windows, Intel Xeon CPU 5160 @ 3.00 GHz, 4.00 GB of RAM	Temperature: 20ºC, 0.1 m/s, 0.01 m^2 jet area zero-gradient boundary conditions on solid surfaces for He mass fraction, wall functions for velocity, k and ε, symmetry boundary conditions at symmetry plane, inflow boundary conditions at the source, no diffusion across source surface, at other open surfaces of domain value for normal velocities calculated from mass balance (constant pressure), for other variables zero-gradient if outflow or given value (equal to the one at time 0) for inflow
UPM	Extended domain in the x and z direction by 50 % 320.272 hexahedral cells. Resolution near the source: 0.044 m. Maximum cell size: 0.37 m.	Time step: 0.1 sec. System clock time: 80 hr 4 CPU Intel Xeon 2,66 GHz	Temperature: 20ºC, Jet inlet: $3.2 \cdot 10^{-4}$ kg/s, 0.02 m^2 jet area, Log law for garage walls, Boundary conditions at open surfaces: fixed ambient pressure ($1.013 \cdot 10^5$ Pa)
UU	Symmetry assumption (half garage), extended domain by 2 m in x direction Case 1: 90x30x58 CVs in x, y and z direction (158.826 CVs totally), 8x22 CVs at vents, 2x2 CVs at the source Case 2: 203.886 CVs totally, 20x22 CVs at vents Case 3: 201.426CVs totally, 20x22 CVs at vents	Constant time step (dt=0.2 sec) with varying number of iterations (50 iter/time step for 0-200 sec, 35 iter/time step for 200-500 sec, 25 iter/time step for >500 sec)	H_2 inflow: temperature T=25^{0}C, H2 inflow: area 0.01 m^2, velocity 0.1 m/s (m_{HE}=1.637·10^{-4} kg/s). Ambient atmosphere: gauge pressure p=0 Pa at the boundaries, temperature T=25^{0}C. Garage walls: non-slip, adiabatic,

		System clock: ~72 hr (Intel Core2Duo 4-core 2.66 GHz)	impermeable, log-law (standard wall functions)

4 RESULTS AND DISCUSSION

Figure 2 and Figure 3 show the predicted and experimental concentration series for Case 1. An oscillatory pattern is observed in the results of DNV and JRC, especially for the lower sensors. DNV commented that these oscillations could be characteristic of the small size of the lower vent as their results of the other cases did not show such large oscillations. DNV repeated the simulation reducing the time step from 0.01 to 0.001 seconds and found no improvement. The reason for the DNV oscillations was also attributed to the fact that FLACS code is mainly developed for high flow rate leaks. JRC attributed the observed oscillations to the numerics but also to the physics of buoyant flows. More specifically JRC observed that even if the flow out of the leak was constant, the helium plume which was developed changed its shape periodically and created varying helium concentrations at probe locations. Oscillations were always found to have the largest amplitude at sensor 1 which is closest to the release location in vertical direction. Case 1 was also simulated by JRC using the Shear Stress Transport (SST) turbulence model. Results obtained were very similar to the laminar calculation. Oscillations also existed but were weaker, so the turbulence model also plays a role. JRC justified their selection of laminar model to the existence of regions inside the garage with almost stagnant flow conditions. Grid sensitivity studies were made by DNV and JRC. DNV reported small changes in the results when the number of CVs was increased by a factor of 8. Mesh refinement at sensible locations (ventilation openings and close to leak) was also performed at JRC. The number of grid nodes was increased by about 30000 to 109600. However, simulation results based on the laminar approach did not change. UU repeated the simulation reducing the time step from 0.2 to 0.05 seconds and found no difference. A time step of 0.2 sec was used for the rest of the cases. NCSRD used in this work a more uniform grid than in [3] (expansion ratio inside the garage is now 1.01 to 1.02) and obtained slightly improved results for the lower sensors. NCSRD performed sensitivity tests to examine the effect of the size of the extra computational volume outside the garage and the effect of the symmetry assumption. For the first case one test was done subtracting the extra volume outside the garage in the y direction while keeping the extra volume in the x and z directions. Another test was done subtracting the extra volume in the z direction but keeping the extra volume in the x and y directions. The results showed oscillations especially in the lower sensors for both tests. In all cases constant pressure boundary condition was used at the free boundaries. For the NCSRD results presented herein and in [3] the domain boundaries were far enough from the vent openings, so no oscillations appear. Regarding the symmetry assumption a simulation was performed with the whole garage geometry and found that this did not result in any change in the results. Regarding the significance of the domain size DNV also reported slow convergence to steady state with a size of the domain equal to that of the garage, which led them to extent their domain by 10% of the garage length in the x direction. However, apart from NCSRD, the domain of the rest of the partners was extended only in the x or in x and z directions from the garage boundaries see Table 2. This could be a reason for the observed differences in concentration levels.

Figure 6 and Figure 7 show the predicted and experimental concentration series for Case 2. Oscillation patterns are observed mainly in the results of JRC but the effect is reduced compared to Case 1. DNV results also showed oscillations but these are reduced significantly compared to Case 1. DNV repeated the simulations deactivating the turbulence model. The predictions were more unstable but the effect was reported as not very significant.

Figure 10 and Figure 11 show the predicted and experimental concentration series for Case 3. Oscillations are repeated in the results of JRC but again the effect was reduced compared to Case 1. Slight oscillations appear in the DNV results. The case was repeated with reduced time step (0.001 seconds). Again the reduction did not produce any change. JRC also performed a calculation with a low Re number extension of the SST turbulence model. The mesh in the garage was modified to

resolve the boundary layer on walls and on the vehicle. The predictions for the two upper sensors in the garage were compared to the laminar calculation but did not show a different time history. DNV reported an unphysical recirculation of He from the upper vent to the lower which disappeared by extending the domain by 55% of garage length in the x direction and by using "nozzle" boundary conditions at the free domain planes.

In order to quantitatively evaluate the results of the participants the mean experimental and simulated concentrations were calculated. The initial period of the release (0 to 1.000-2.000 seconds depending on the case) was not taken into account as the nearly steady-state concentration values were of interest. These values are presented in Table 3. The results of UU partner were given for 2.000 seconds; particularly for Case 1 it was not assured that nearly steady state conditions were achieved. However, for comparison reasons, all results by UU are included. Figure 4, Figure 8 and Figure 12 show the ratio of predicted (C_p) to experimental (C_o) mean concentrations of the partners for each sensor and each case.

As can be seen from the figures and the table, there is a general tendency to over-predict the experimental results for Case 1. Specifically, for Sensor 1 $(C_p/C_o)_{NCSRD}$=0.9 whereas for the rest of the partners the ratio was $3<C_p/C_o<7$, for Sensors 2 and 3 the over prediction was not higher than 1.3 for all partners and for Sensor 4 $(C_p/C_o)_{NCSRD}$=1.8 and for the rest of the partners $4<C_p/C_o<6.5$. One of the parameters reported by the partners was the fresh air inflow rate in air changes per our (ACH). For this case DNV and JRC reported 3.77 ACH whereas NCSRD reported 1.62 ACH.

For the case with the smallest vent openings, NCSRD results were closer to the experimental than the rest of the partners. It is believed that the lesser height of the vent openings the greater the effect of the extension of the domain in the x, y and z directions and the uniform grid on the concentration levels particularly at the lower sensors.

For Case 2, there is again a general tendency to over predict the experimental results. Specifically, for Sensor 1 the results of JRC, UPM and UU were higher ($2<C_p/C_o<2.5$) whereas for NCSRD and DNV the results were lower than the experimental ($(C_p/C_o)_{NCSRD}$=0.25, $(C_p/C_o)_{DNV}$=0.56). For Sensors 2 and 3 the C_p/C_o was not higher than 1.5. For Sensor 4 all partners over predicted the experimental ($(C_p/C_o)_{NCSRD}$=1.67, $(C_p/C_o)_{DNV}$=4.3, $(C_p/C_o)_{UPM}$=4.8, $(C_p/C_o)_{UU}$=6 and $(C_p/C_o)_{JRC}$=8.5). The reported fresh air inflow was 6.73 ACH for JRC, 7.81 ACH for DNV and 4.85 ACH for NCSRD.

For Case 3 the partners either over predicted $(C_p/C_o)_{JRC}$=2.2, $(C_p/C_o)_{UU}$=1.8, or under predicted $(C_p/C_o)_{NCSRD}$=0.09, $(C_p/C_o)_{DNV}$=0.1 whereas UPM results were very close $(C_p/C_o)_{UPM}$=1.05 for Sensor 1. For Sensors 2 and 3 the results of all partners were close to the experimental ($0.8<(C_p/C_o)<1.3$) whereas for Sensor 4 all partners over predicted the experimental ($(C_p/C_o)_{NCSRD}$=1.6, $(C_p/C_o)_{DNV}$=2, $(C_p/C_o)_{UPM}$=5.7, $(C_p/C_o)_{UU}$=12 and $(C_p/C_o)_{JRC}$=15). The reported fresh air inflow was 8.08 ACH for JRC, 10.77 ACH for DNV and 6.25 ACH for NCSRD.

Generally, the overall results were worse for the lower sensors than the upper sensors. This could be attributed to experimental uncertainty at the lower sensors because of the low concentration levels (the accuracy of the measurements was not reported by experimentalists). Additionally, some of the experimental results were not completely stable. Another issue was that the repeatability of experimental results was also not reported. Lastly, the environmental conditions were not given. Partners assumed different temperature as initial condition (see Table 2). To make a safer conclusion on the comparison between the experimental and the numerical results information on these conditions were necessary.

Table 3: Mean experimental and simulated concentrations (vol. %)

	Experimental (C_o)	DNV (C_p)	JRC (C_p)	NCSRD (C_p)	UPM (C_p)	UU (C_p)
Case 1	S1:0.21, S2:2.48,	1.50,2.92,	1.15,2.90,	0.19, 2.55	0.81, 2.99	0.98, 3.01

	S3:2.35, S4:0.28	2.94,1.81	2.95, 1.49	2.56, 0.50	2.98, 1.18	3.02, 1.33
Case 2	S1:0.16, S2:1.41, S3:1.32, S4:0.06	0.09,1.47, 1.49,0.26	0.41, 1.86 1.92, 0.51	0.04, 1.36 1.38, 0.1	0.32, 1.58 1.65, 0.29	0.34,1.59, 1.64,0.36
Case 3	S1:0.20, S2:1.28, S3:1.20, S4:0.03	0.02,1.11, 1.04,0.06	0.44, 1.57 1.62, 0.46	0.02, 1.17 1.18, 0.05	0.21, 1.06 1.06, 0.17	0.36,1.30, 1.30,0.36

One parameter for assessing the risk of an accidental release is the flammable mixture volume which is the volume of the air-hydrogen mixture, where hydrogen concentration is within the lower and upper flammability limits (4 to 75%). Figure 5, Figure 9 and Figure 13 show the predicted flammable mixture volume (JRC, NCSRD and UPM) and mass (JRC and NCSRD) time series for Case 1, 2 and 3 respectively. The higher predictions were given by JRC, following UPM whereas the lowest are given by NCSRD. Oscillations are again shown in JRC results. For Case 1, the mean value of the flammable volume for JRC was 0.16 m^3, for UPM the flammable volume was 0.15 m^3 and for NCSRD 0.04 m^3. The differences can be attributed to the differences in the concentrations between these partners as revealed by the comparison of the previous graphs. The flammable cloud was located under the front of the vehicle and extended in the z-direction in front of the vehicle in a thin column-like shape. The rest of the garage mixture remained leaner than the LFL of H_2. For Case 2, the mean value of the flammable volume for JRC was 0.15 m^3, for UPM 0.09 m^3 and for NCSRD 0.03 m^3. Increasing the height of the vents by 4 times resulted in a decreased flammable volume. Most of the garage mixture had a concentration less than the LFL of H_2 while the increase of the vent size resulted in a flammable cloud from the leak that slightly extended beyond the underside of the front of the vehicle. For Case 3, the mean value of the flammable volume for JRC was 0.18 m^3, for UPM 0.09 m^3 and for NCSRD 0.037 m^3. This time, increasing the height of the vents did not decrease the flammable volume further even though the reported volumetric flow rates of air entering the garage were increased compared to the previous cases. In the simulations of NCSRD calculations of the volumetric flow rate entering or leaving each vent were done. These calculations revealed that for Case 1, 2 and 3 only fresh air entered the lower vent whereas the mixture of air with He exited only from the upper vent. However, only in Case 3, fresh air entered the garage from the upper vent too possibly due to the fact that in this case the vents were quite large. Thus, the fresh area entering from the upper vent for this case hindered the outflow of the He-air mixture causing the flammable volume inside the garage not to decrease as compared to Case 2.

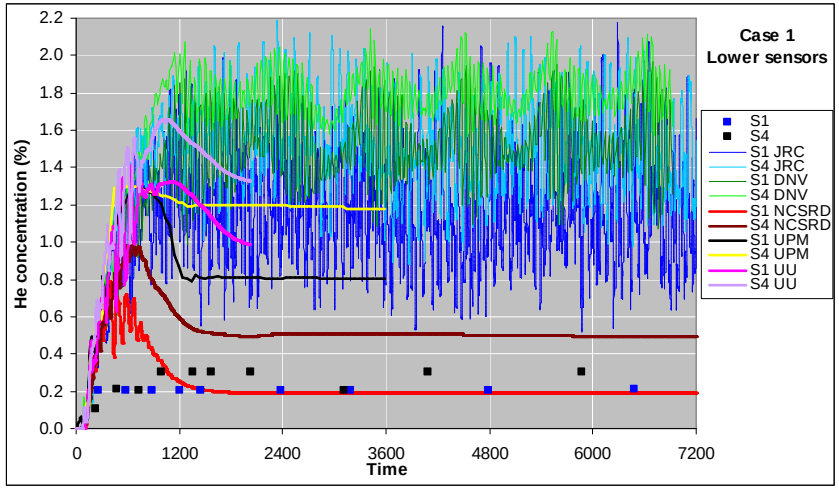

Figure 2: He concentration (vol. %) histories for Case 1, lower sensors

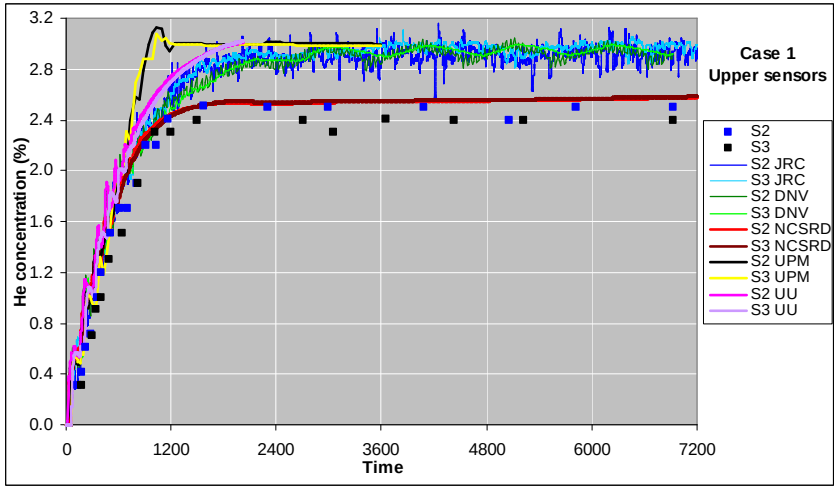

Figure 3: He concentration (vol. %) histories for Case 1, upper sensors

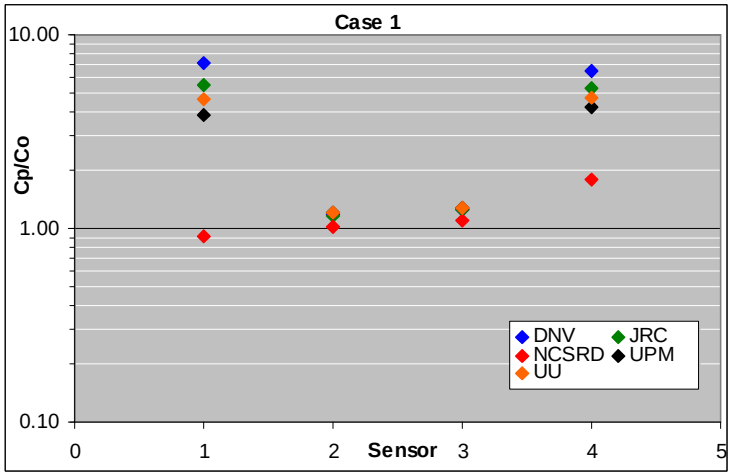

Figure 4: Predicted to experimental mean hydrogen concentration ratio

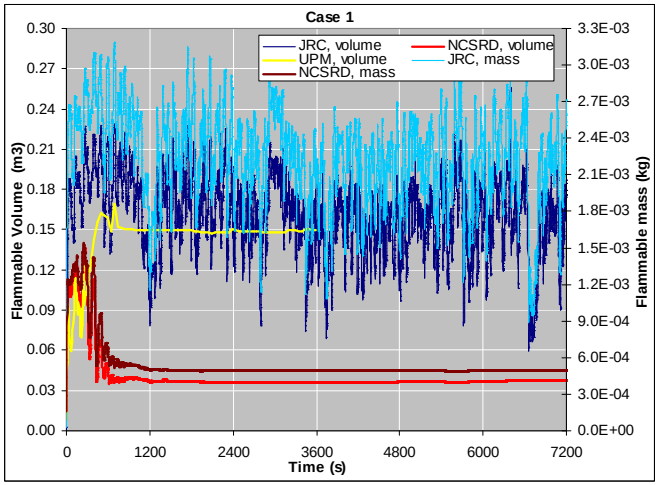

Figure 5: Predicted flammable mixture volume and H2 mass histories

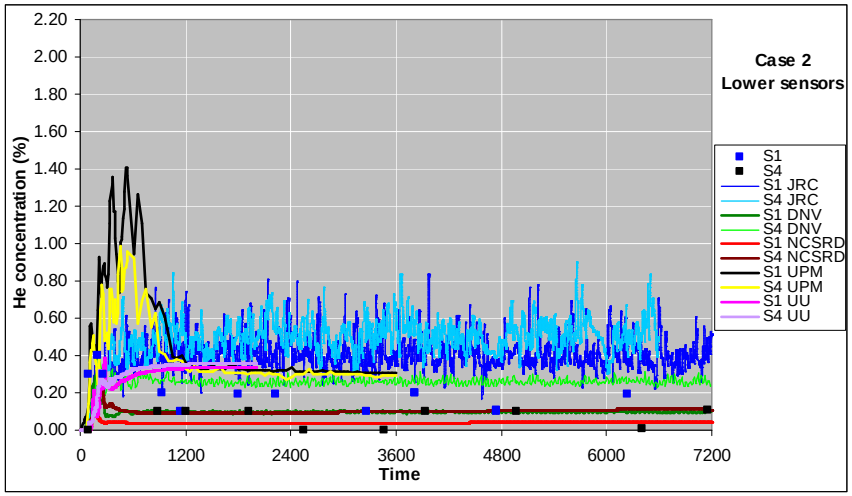

Figure 6: He concentration (vol. %) histories for Case 2, lower sensors

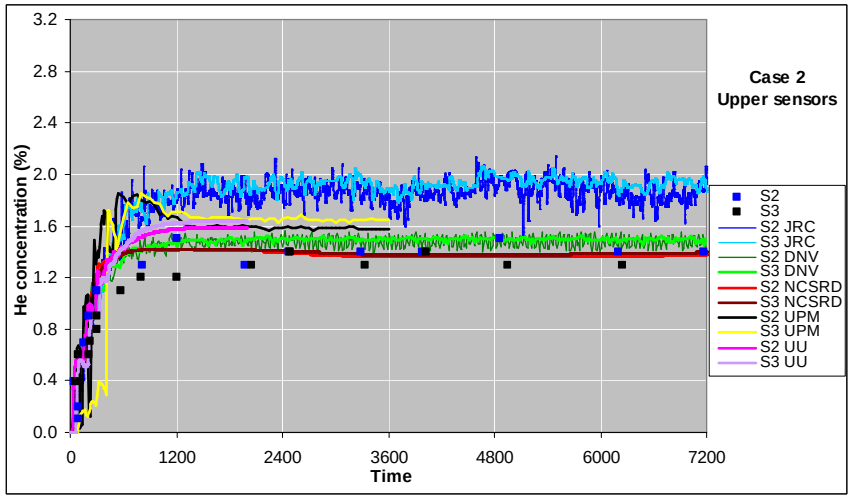

Figure 7: He concentration (vol. %) histories for Case 2, upper sensors

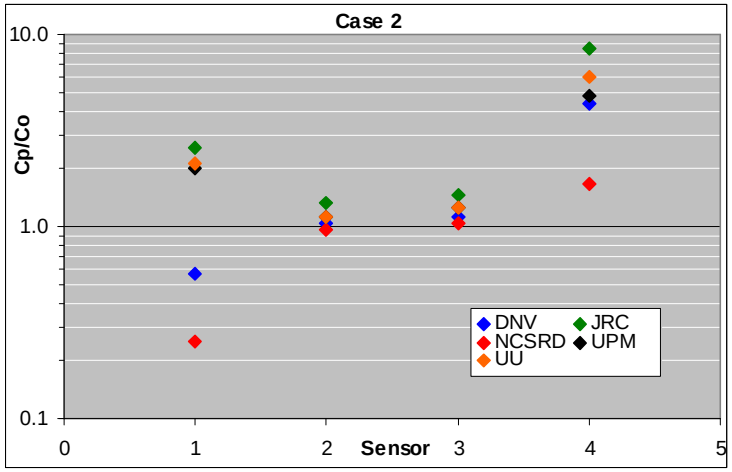

Figure 8: Predicted to experimental mean hydrogen concentration ratio

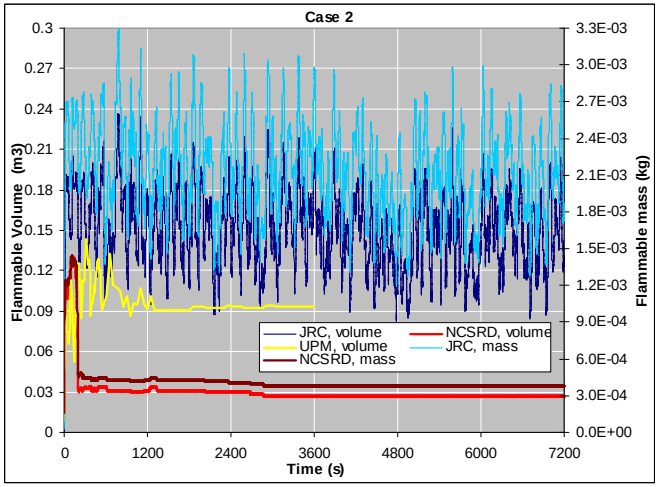

Figure 9: Predicted flammable mixture volume and H2 mass histories

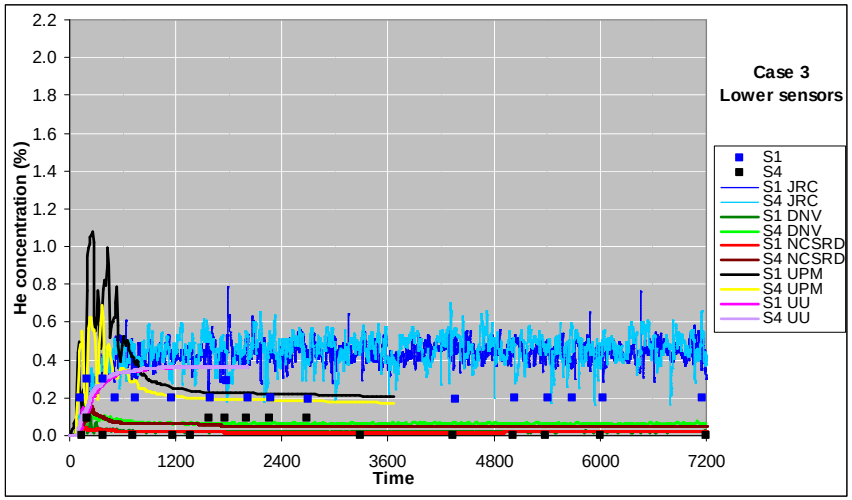

Figure 10: He concentration (vol. %) histories for Case 3, lower sensors

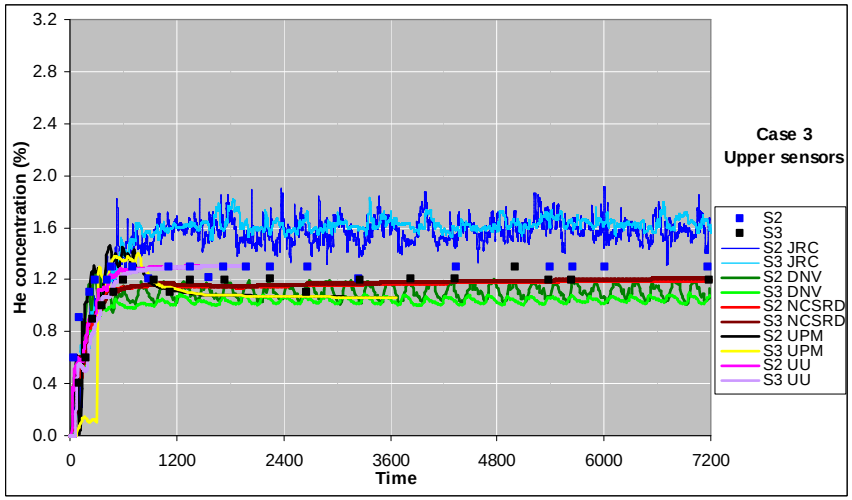

Figure 11: He concentration (vol. %) histories for Case 3, upper sensors

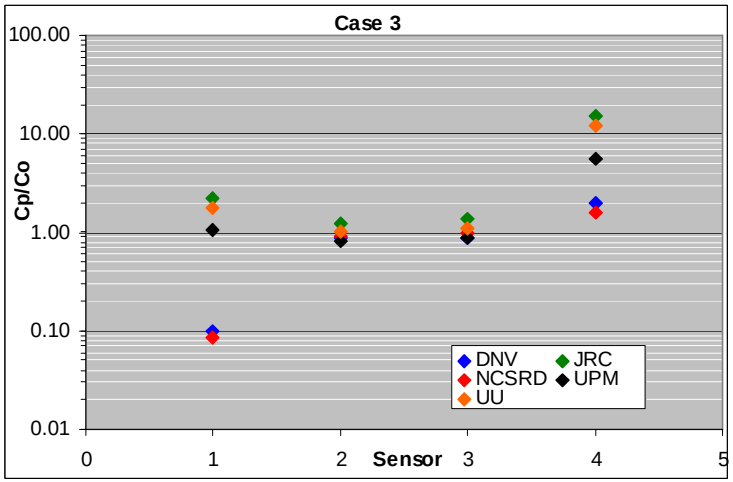

Figure 12: Predicted to experimental mean hydrogen concentration ratio

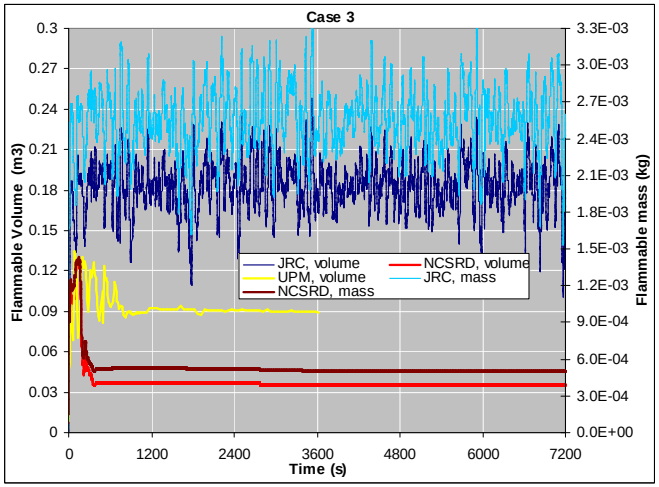

Figure 13: Predicted flammable mixture volume and H2 mass histories

5 CONCLUSIONS

A comparison between the experimental and numerical results of the SBEP V20 of WP6 of HySAFE was presented. Five HySAFE partners participated in this benchmark with 4 different codes (ADREA-HF, CFX, FLACS and FLUENT) using different models (k-e, laminar, SST, low Re number SST). This study compared the results predicted by the partners to the experimental measurements with an attempt to assess and validate the performance of the codes and models. Furthermore, the effect of passive ventilation on the formation of flammable cloud was investigated.

The submitted results can be categorized into either oscillatory concentration histories or non oscillatory. One probable reason for the appearance of the oscillations is the proximity of the free planes to the boundaries of the garage. It was found that when these planes were far enough from the garage, the oscillations did not appear. Other possible reasons could be the selection of the turbulence model and the numerics.

General agreement between the partners' predictions and the experimental data was good with tendency to overestimate the results of the upper sensors for the small and medium vent sizes and under estimate for the large vent size. Laminar model over estimates more than k-e model the experimental data, as expected due to the lower diffusion. Disagreements in the results of the lower sensors could be attributed to experimental uncertainties due to the low concentration levels.

Concerning the flammable mixture volume in the garage, increasing the height of the vents by 4 times resulted in a decreased flammable volume. A further increase of the height by 2 did not decrease the flammable cloud more. For this case it was found that fresh air not only entered the garage from the lower vent but also from the upper thus hindering the outflow of the mixture He-air from the upper vent.

6 ACKNOWLEDGMENTS

The authors would like to thank the European Commission for co-funding of this work in the framework of the HySafe FP6 Network of Excellence (contract no. SES6-CT-2004-502630).

7 REFERENCES

[1] HySAFE, Safety of hydrogen as an energy carrier, Network of Excellence, FP6, Available from: www.hysafe.org, **2003-2009**

[2] Swain, M. R., Grilliot, E. S. and M. N. Swain, Phase 2: Risks in indoor vehicle storage, in Addendum to Hydrogen Vehicle Safety Report: Residential Garage Safety Assessment, analysis conducted by: Michael R. Swain, University of Miami, under subcontract to Directed Technologies Inc, prepared for the Ford motor company under prime Contract No. DE-AC02-94CE50389 to the U.S. Department of Energy, Office of Transportation Technologies, August **1998**

[3] Papanikolaou, E.A. and Venetsanos A.G., "CFD modelling for helium releases in a private garage without forced ventilation", 1st International Conference on Hydrogen Safety, Pisa, September, **2005**

[4] Swain, M. R., Grilliot, E. S. and M.N. Swain: Experimental verification of a hydrogen risk assessment method, Chemical Health and Safety, **1999**, pp. 28-32

[5] Agranat, V., Cheng, Z. and Tchouvelev, A., CFD Modelling of Hydrogen Releases and Dispersion in Hydrogen Energy Station, Proceeding of WHEC-15, **2004**, Yokohama

[6] Swain, M.R. and Shriber J., "Comparison of hydrogen, natural gas, liquefied petroleum gas and gasoline leakage in a residential garage", Energy and Fuels, 12, pp.83-89, **1998**

[7] Breitung, W., Necker, G., Kaup, B. and Veser, A., Numerical simulation of hydrogen in a private garage, Proceedings of the fourth international symposium on hydrogen power–theoretical and engineering solutions–Hypothesis IV, Stralsund (Germany), 9-14 September **2001**

[8] Support facilities for hydrogen fuelled vehicles-Conceptual design and cost analysis study, Technical report, **2004**, Prepared for California Fuel Cell Partnership by Parsons and Brinckerhoff in association with TIAX and University of Miami

[9] Paillere, H., Studer, E., Beccantini, A., Kudriakov, S., Dabbene, F. and Perret C., "Modelling of H2 dispersion and combustion phenomena using CFD codes". 1st International Conference on Hydrogen Safety, Pisa, September, **2005**

[10] Barley, C.D., Gawlik, K., Ohi, J. and Hewett, R., "Analysis of buoyancy-driven ventilation of hydrogen from buildings", 2nd International Conference on Hydrogen Safety, San Sebastian, Spain, 11-13 Sept., **2007**

[11] Gupta, S., Brinster, J., Studer, E. and Tkatschenko I., "Hydrogen related risks within a private garage: concentration measurements in a realistic full scale experimental facility", 2nd International Conference on Hydrogen Safety, San Sebastian, Spain, 11-13 Sept., **2007**

[12] Lowesmith, B.J., Hankinson, G., Spataru, C. and Stobbart M., "Gas build-up in a domestic property following releases of methane/hydrogen mixtures", 2nd International Conference on Hydrogen Safety, San Sebastian, Spain, 11-13 Sept., **2007**

[13] Lacome, J.M., Dagba, Y., Jamois, D., Perrette, L. and Proust Ch., "Large-scale hydrogen release in an isothermal confined area", 2nd International Conference on Hydrogen Safety, San Sebastian, Spain, 11-13 Sept., **2007**

[14] Venetsanos, A.G., Papanikolaou, E., Delichatsios, M., Garcia J., Hansen, O.R., Heitsch, M., Huser, A., Jahn, W., Jordan, T., Lacome, J.-M., Ledin, H.S., Makarov, D., Middha, P., Studer, E., Tchouvelev, A.V., Teodorczyk, A., Verbecke, F. and Van der Voort, M.M., An inter-comparison exercise on the capabilities of CFD models to predict the short and long term distribution and mixing of hydrogen in a garage", International Journal of Hydrogen Energy, doi: 10.1016/j.ijhydene.2009.01.055, **2009**

[15] K.Papakonstantinou, A.Chaloulakou, A.Duci, N.Vlachakis and N.C.Markatos, "Air quality in an underground garage: computational and experimental investigation of ventilation effectiveness", Energy and Buildings, Vol.35, Issue 9, pp.933-940, October 2003

[16] A.Duci, K.Papakonstantinou, A.Chaloulakou and N.C.Markatos, "Numerical approach of carbon monoxide concentration dispersion in an enclosed garage", Building and Environment, Volume 39, Issue 9, pp. 1043-1048, September 2004

[17] http://www.gexcon.com

[18] ANSYS Inc., Southpointe, 275 Technology Drive Canonsburg, USA, http://www.ansys.com/products/cfx.asp

[19] http://www2.ipta.demokritos.gr/pages/ADREA-HF.html

[20] FLUENT code http://fluent.com/software/fluent/